VERTICAL DISTRIBUTION OF CLOUD LIQUID WATER AND ICE: A COMPARISON OF MODIS SATELLITE OBSERVATIONS AND THE GISS GLOBAL CLIMATE MODEL

A Thesis

by

KATHERINE LORAINE PITTS

Submitted to the Office of Graduate and Professional Studies of
Texas A&M University
in partial fulfillment of the requirements for the degree of

MASTER OF SCIENCE

Chair of Committee,	Shaima Nasiri
Committee Members,	Ping Yang
	Kenneth Bowman
	Andrew Klein
Head of Department,	Ping Yang

May 2015

Major Subject: Atmospheric Sciences

ABSTRACT

Clouds continue to be a large source of uncertainty within global climate models. While satellites provide the only global datasets for comparison with these models, satellite retrievals provide inferences of cloud properties, rather than direct measurements. Therefore, comparisons between climate model simulations and satellite retrievals require careful construction of globally-gridded and time-averaged (Level 3) satellite datasets. For some types of comparisons, existing Level 3 datasets may not be sufficient, necessitating the generation of gridded datasets directly from Level 2 products.

The current study uses a filtering and gridding algorithm to create a customized globally-gridded (i.e., Level 3) dataset based on Aqua MODIS Level 2 cloud top pressure and cloud optical property retrievals. With the recent release of MODIS Collection 6, we utilize this algorithm to examine the differences between cloud parameters in the MODIS Collection 5 and Collection 6 datasets, and then compare these satellite measurements to the GISS-E2-H model-simulated cloud parameters that were provided for the Coupled Model Intercomparison Project - Phase 5 (CMIP5). This comparison study focuses on the vertical distribution of cloud liquid water and ice, especially in the mid-troposphere where mixed-phase clouds are most likely to occur.

Results show that the cloud retrieval algorithm improvements with MODIS Collection 6 lead to an overall decrease in uncertainty in cloud water path retrievals, as well as a change in the vertical distribution of clouds (high clouds higher, low clouds lower) and the resulting vertical distribution of cloud water path (increased mid-level cloud water path). When MODIS Collection 6 data are compared with GISS-E2-H climate model simulations, it is clear that the model greatly overestimates ice wa-

ter path within a double ITCZ (intertropical convergence zone) in the high cloud height regime, but underestimates ice water path in higher latitudes. The model also overestimates low level liquid water path over land, especially over mountainous regions.

The filtering and gridding algorithm used in this study is a convenient tool for building custom gridded datasets to address research questions that the official Level 3 datasets were not designed for.

ACKNOWLEDGEMENTS

We acknowledge the World Climate Research Programme's Working Group on Coupled Modelling, which is responsible for CMIP, and we thank the climate modeling groups (described in section 2.1.2 of this paper) for producing and making available their model output. For CMIP the U.S. Department of Energy's Program for Climate Model Diagnosis and Intercomparison provides coordinating support and led development of software infrastructure in partnership with the Global Organization for Earth System Science Portals.

Funding for this research was primarily provided by NASA Grant NNX10AP06G, with initial algorithm development funding by NASA Grant NNX11AO55G.

TABLE OF CONTENTS

LIST OF FIGURES

FIGURE Page

LIST OF TABLES

1. INTRODUCTION

Clouds are the main modulators of the global radiation budget, yet models still have trouble simulating them, causing large uncertainties in global climate model projections. The vast range of cloud sizes in both the horizontal and vertical extents makes modeling them difficult, especially if the cloud size is smaller than the model grid size. Additionally, cloud composition (ice, liquid water, or mixed-phase), cloud fraction, cloud height, and cloud optical depth are all factors that affect the cloud-radiative feedback.

Comparisons of model-simulated cloud variables with equivalent satellite cloud products are the best way to start diagnosing the differences between model output and observations. Satellites provide the only global observational datasets of cloud properties; however, satellite retrievals provide inferences of cloud properties rather than direct measurements. Therefore, comparisons between climate model simulations and satellite retrievals require careful construction of globally-gridded and time-averaged, i.e., Level 3, satellite datasets.

Official Level 3 datasets are filtered and gridded per the instrument team's discretion, meaning lack of choice for the end user. If a product user needs a dataset averaged over a different space or time resolution they could resample the Level 3 dataset, but that may bring unknown or untraceable errors. Likewise, a user might need a dataset to be filtered differently for quality control purposes, or to be able to focus on a particular science question that the Level 3 product was not designed to address. Therefore, for some types of comparisons, existing Level 3 datasets may not be sufficient, necessitating the generation of datasets gridded directly from the geophysical properties retrieved at the instrument resolution, i.e., from Level 2 satellite

products.

1.1 Clouds and Climate

The Intergovernmental Panel on Climate Change Fifth Assessment Report (IPCC AR5; Stocker et al. 2013) was recently released along with the Coupled Model Intercomparison Project - Phase 5 (CMIP5) global climate model output that are the basis of the IPCC report. Model-satellite comparison studies have been performed and show that while the CMIP5 models overall are better at simulating cloud processes than their predecessors in the CMIP3 (Jiang et al., 2012), there is still great uncertainty in the climate feedback values due to clouds, mainly from the cloud radiative effect (CRE) (Stocker et al., 2013). Boucher et al. (2013) summarize that current global measurements of the CRE indicate an annual shortwave CRE of about -50 W m^{-2} and a longwave CRE of +30 W m^{-2}. The net CRE of -20 W m^{-2} implies a radiative energy loss, and thus a cooling of the current climate, due to the presence of clouds. The net CRE calculated by models depends on how those models parameterize the properties that govern the shortwave and longwave CREs. Individual CMIP5 models produce a wide range of shortwave and longwave CRE values, which cause a large spread in the net CRE values (roughly from -15 to -35 W m^{-2}) (Flato et al., 2013; Bony et al., 2011; Dolinar et al., 2014). Understanding the model biases in CRE requires a better analysis of the model biases in moist processes and cloud properties, including cloud fraction, vertical distribution of clouds, and cloud liquid water and ice content (Flato et al., 2013; Bony et al., 2011; Su et al., 2013).

Model-satellite comparison studies of these cloud properties compare the "historical" CMIP5 model runs, which are representations of the recent climate (Taylor et al., 2012), to satellite cloud observations, such as those from the Moderate-resolution Imaging Spectroradiometer (MODIS), the Cloud-Aerosol Lidar and In-

frared Pathfinder Satellite Observation (CALIPSO), and/or the CloudSat Level 3 cloud products. One of the main findings is that the mean ice water content and path tend to be overestimated by the models, especially with the Goddard Institute for Space Studies (GISS) models (Jiang et al., 2012; Li et al., 2012). This is likely associated with the fact that the amount of high clouds are overestimated by models, whereas the low and mid clouds are underestimated (Cesana and Chepfer, 2012). The models show similar spatial patterns of ice clouds (typically high clouds) to what is seen in satellite observations (Li et al., 2012), but the models do not simulate the spatial patterns of low and mid clouds very well (Jiang et al., 2012). Individual models produce very different vertical distributions of cloud water content, especially so with the ice water content (Li et al., 2012); however, the multi-model means tend to simulate vertical structures similar to satellite observations (Jiang et al., 2012).

Regarding moist processes, the individual models simulate the vertical distribution of water vapor better than they simulate cloud properties (Jiang et al., 2012). In comparison to Atmospheric Infrared Sounder (AIRS) satellite humidity profiles, Tian et al. (2013) show that the CMIP5 models are too dry in the tropical lower troposphere but too moist in the tropical upper troposphere and extratropical troposphere, especially over the southern hemisphere. The CMIP5 models also have the double-ITCZ (intertropical convergence zone) problem that persists in the coupled global climate models, likely due to the models being too dry over the equatorial convective regions while also too moist just off the equator.

The GISS models stand out with great overestimations of cloud ice water content compared to satellite observations, especially along the ITCZ. Most of the difference occurs above the mid-troposphere where there are mainly ice clouds (Li et al., 2012; Jiang et al., 2012). These models' positive bias in cloud ice water content in the tropics is due to compensation for a negative bias in clouds and cloud ice water

path in the extratropics while also keeping the globally averaged radiation budget consistent with observations (Li et al., 2012).

Other CMIP5 models also have adjusted, or "tuned," cloud properties to ensure the correct net global radiation budget is simulated. For example, a model could be tuned by increasing the amount of ice clouds to increase the longwave CRE, or by making low clouds more optically thick to compensate for the underestimation of low cloud amounts and thus increasing the shortwave CRE (Cesana and Chepfer, 2012; Nam et al., 2012). The CMIP5 models do a reasonable job of simulating the large-scale dynamic and thermodynamic variables that interact with the cloud parameterization schemes, since those large-scale variables are constrained by the global energy balance, but the subgrid cloud parameterizations produce results that differ significantly from observations and vary greatly from model to model (Su et al., 2013).

Although the CMIP5 generation models have improved their cloud simulation parameterizations, there is continued need to validate the model simulations of cloud variables with observations and determine where the models fall short of simulating reality. The studies referenced here have already contributed greatly to this investigation. The current study proposes to perform similar research, but to approach the problem differently with a focus on the satellite datasets that are being used for comparison with models.

1.2 Objectives

To determine model biases in CRE, a more in-depth analysis needs to be done on cloud fraction, vertical distribution of clouds, and cloud liquid water and ice content. This study's first objective, therefore, is to use Aqua MODIS observations to quantify the vertical distributions of liquid water and ice clouds. Aqua MODIS is

a well-calibrated satellite instrument that provides just over a decade of global cloud measurements. This first task also includes an investigation of cloud fraction, as this quantity will be necessary for performing satellite-model comparisons.

This study's second objective is to use the results from the first objective to then compare Aqua MODIS observations of clouds in different height regimes to cloud parameters simulated by global climate models to determine where, vertically, the models can use improvements and/or apply constraints based on observations.

The aforementioned satellite-model comparison studies took advantage of official Level 3 satellite products. These products are easily obtainable and accessible by users of all experience levels because they are globally-gridded and time-averaged, and come in fewer and more compact files as compared to the Level 2 products. On the other hand, the Level 3 products are filtered and gridded per the instrument science team's discretion, meaning lack of choice for the end user. This one-size-fits-all approach is not ideal for this study's objectives.

This study therefore uses a uniform space-time gridding algorithm (hereafter, STG) produced by Smith et al. (2013) to create a customized globally-gridded dataset based on Aqua MODIS Level 2 cloud parameter data for use in comparison with the model-simulated cloud parameters that were provided for the CMIP5. Using the STG to create a custom global dataset, rather than using the official Level 3 datasets that other studies have used, means greater control over data filtering techniques, quality assurance, and statistics generated in the final product. One of these filtering techniques is to assign height values to cloud products, which is not provided in the official MODIS Level 3 dataset. Classifying cloud products to certain height regimes is of great importance to this study's objectives, and the methodology presented in Chapter 2 describes how this is achieved. This is followed by results in Chapter 3, and conclusions in Chapter 4.

2. DATA AND METHODS

2.1 Uniform Space-Time Gridding

The uniform space-time gridding (STG) algorithm allows a user to create daily gridded datasets from any polar-orbiting or geostationary satellite Level 2 products. The daily grids can then be averaged up to a longer time-averaged dataset. The space gridding portion of the algorithm is implemented first and is where a user can set filters such as grid size, satellite viewing zenith angle, sun zenith angle, quality flag, and specifications on what measurements are to be included. Once these filters are set, the satellite observations are gridded to the user-specified grid by assigning each observation to its nearest neighbor grid cell. By assigning all observations to a grid cell, the number of observations per grid cell can be kept track of for statistical purposes. Once the space gridding is complete, all data that were not included by the filters are discarded. This is a data reduction technique that speeds up the analysis of the newly gridded data during the time gridding phase.

The time gridding part of the algorithm includes statistical analysis of the newly gridded datasets. First, daily statistics determine number of measurements, mean, and variance, among other possibilities. The number of observations in each grid cell that do not have a value of zero is defined as a measurement, and these measurements are averaged to produce one mean value per grid cell for that day. These daily gridded products can then be aggregated into a longer time-averaged product (e.g., a monthly dataset).

2.1.1 STG filtering for MODIS satellite data

In this study, the original STG developed by Smith et al. (2013) has been optimized to significantly decrease computer processing time during the space gridding,

and to allow for additional filtering options to be implemented. The STG is being used in this study to filter and grid cloud water path (CWP) data from Aqua MODIS Level 2 Collection 5 (C5) and Collection 6 (C6) datasets (MYD06_L2; GSFC 2014) for the month of May over the years 2003 - 2012. These years provide the longest overlapping time between Aqua MODIS observations (available July 2002 - present) and the CMIP5 models' historical runs (available 1850 - 2012). Only one month was chosen for this study due to the computational time required to run the filtering process. The MODIS filtering and gridding setup is listed in Table 2.1.

Table 2.1: STG filtering setup for MODIS Level 2 C5 and C6 CWP data.

Filtering Parameter	Filter Value
Space Grid Filtering	
Grid size	$2^\circ \times 2^\circ$
Viewing zenith angle	$\leq 32^\circ$
Sun zenith angle	$\leq 90^\circ$
CWP Quality Control Filtering Cases	
Confidence (C5 only)	3 (best)
Uncertainty	$\leq 80\%$
Height Regime Filtering Cases	
All	No CTP filtering
High	$440 \geq$ CTP $>$ 50 hPa
Mid	$680 \geq$ CTP $>$ 440 hPa
Low	$1000 \geq$ CTP $>$ 680 hPa
Time Grid Filtering	
Min. no. pixels threshold	$>$ 1.5 STD(mean obs)

For the space gridding, a grid size of $2^\circ \times 2^\circ$ was chosen to produce a resolution similar to those used in global climate models. The satellite viewing zenith angle filter was set to keep pixels within $\leq 32^\circ$, which is typical for satellite studies so as to avoid artifacts from pixel growth and longer atmospheric paths at larger viewing angles. A sun zenith angle filter of $\leq 90^\circ$ was set to keep only daytime pixels since

the CWP variable is an optical cloud retrieval property that relies on observations of reflected solar radiation.

These CWP grids were then further filtered by quality case. The first quality filter is set to keep all the "best" confidence retrieved pixels based on the quality assurance bit assignments (bit 3 = best), and the second is to keep only the pixels with less than 80% uncertainty. The quality assurance confidence filter is only applicable for the MODIS C5 dataset, as the MODIS C6 dataset uses an improved uncertainty quality flag that is to be used in place of the confidence assignments, and sets all successful retrievals to the "best" confidence flag (Platnick et al., 2013; MODIS Atmosphere, 2014).

The CWP data were then broken down by cloud height regime. Because MODIS cloud retrievals are made on the assumption that the satellite is seeing a homogeneous, plane-parallel, single-layered cloud scene, we can then assign each CWP pixel value, which is a column integrated variable, to a specific height using the retrieved cloud top pressure (CTP). The cloud height regimes defined in the STG are *all* (no CTP filtering), *high* ($440 \geq \text{CTP} > 50$ hPa), *mid* ($680 \geq \text{CTP} > 440$ hPa), and *low* ($1000 \geq \text{CTP} > 680$ hPa). In MODIS C5, the CTP data have a 5-km horizontal resolution while the CWP data have a 1-km horizontal resolution. In MODIS C6, there is both a legacy 5-km CTP variable and a new 1-km CTP variable (Menzel et al., 2013; Baum et al., 2012). The algorithm that determines CTP values is independent of the optical property retrieval algorithm that determines CWP values; however, the CTP pixels are indexed and filtered out per the CWP quality filter criteria. This study analyzes each CTP horizontal resolution case to determine how the resolution differences affect the vertical distributions of cloud liquid water and ice.

Lastly, for the time gridding part of the algorithm a minimum number of daily observations threshold was set as 1.5 standard deviations from the monthly mean

number of pixels per grid cell so that only the cells with a significant amount of daily retrieved pixels will be used to calculate a daily average. For instance, if one $2^\circ \times 2^\circ$ grid cell contains 1970 CWP daily observed pixels on average over the month of May, then this algorithm would require that at least 69 CWP pixels (which is 3.5%, or the lower half of 1.5 standard deviations from the mean) be present in that cell for the pixels to be used in the daily statistics. Note that the official MODIS Level 3 product requires just one pixel within each $1^\circ \times 1^\circ$ grid box to compute a grid cell daily average, meaning that those daily grid cell averages, and thus the monthly grid cell averages, are at risk of being geographically misrepresented by a single outlier observation. With the minimum number threshold set as the last filter in this process, the resulting data are used to create a daily average global grid. These daily averages are then aggregated to create monthly average grids, and the monthly grids are aggregated to make a time-series average.

2.1.1.1 Cloud fraction weighting

Before these newly gridded MODIS datasets can be compared to the model simulations, it must be noted that the MODIS observations are measuring only cloudy scenes, whereas the model simulations are representing both clear and cloudy scenes. To compare the two datasets, the MODIS CWP grids must be weighted by cloud fraction.

Cloud fraction in this study is calculated using both the MODIS cloud mask and the cloud property retrievals. First, a cloud mask cloud fraction (CF) is determined by,

$$CF = \frac{\#CM}{\#all}, \tag{2.1}$$

where #CM is the number of pixels that have cloud mask bits that are equal to 0 (confident cloudy) or 1 (probably cloudy). CM is divided by all retrieved pixels to

get the cloud mask cloud fraction.

Then, a liquid fraction (LF) and an ice fraction (IF) are calculated using the number of CWP retrievals from the STG process:

$$LF = \frac{\#LWP}{\#LWP + \#IWP} = \frac{\#LWP}{\#CWP}, \tag{2.2}$$

$$IF = \frac{\#IWP}{\#LWP + \#IWP} = \frac{\#IWP}{\#CWP}, \tag{2.3}$$

where #LWP, #IWP, and #CWP are the number of liquid water path retrievals, ice water path retrievals, and cloud water path retrievals, respectively.

Next, a cloud fraction based on the CWP retrievals for each height regime is calculated:

$$CF_{low} = \frac{\#CWP_{low}}{\#CWP_{all}}, \tag{2.4}$$

$$CF_{mid} = \frac{\#CWP_{mid}}{\#CWP_{all}}, \tag{2.5}$$

$$CF_{high} = \frac{\#CWP_{high}}{\#CWP_{all}}. \tag{2.6}$$

The final cloud fraction is calculated by multiplying the CF, LF or IF, and each individual height regime fraction together. For example, the low-level ice fraction would be determined by,

$$Low\ ice\ fraction = CF * IF * CF_{low}. \tag{2.7}$$

Following a structure similar to Equation 2.7 for each height regime and phase produces the cloud fraction value that is multiplied by the average CWP to get the cloud-fraction-weighted CWP that this study then uses to compare against model output of CWP.

2.1.2 Global climate model data

This study compares the STG custom gridded Aqua MODIS satellite observations to the archived CMIP5 simulations from the GISS-E2-H model, which was produced by the NASA Goddard Institute for Space Studies. The CMIP5 experiment "Historical" and "historicalExt" (extended historical) monthly-averaged model runs (ESGF, 2014) were selected for use, as these are simulations of the recent climate (Taylor et al., 2012). The historical run is simulated for the years 1850 - 2005, and the extended historical run is for 2006 - 2012. This study averages the model-simulated output for the month of May over the years 2003 - 2012 to match the timeline of the gridded MODIS time-series average.

The model variables of interest are the CWP and the cloud water mass fraction, which is integrated to get the CWP values for the defined height regimes. The model's 2.5° longitude $\times$ 2° latitude horizontal grid is interpolated across the longitudes to match the MODIS grid resolution of $2^\circ \times 2^\circ$. The model's vertical resolution for the cloud water mass fraction is in hybrid sigma coordinates, which must be converted, column by column, into pressure coordinates to be able to integrate the cloud water mass fraction to determine the model's CWP value between the pressure levels of the defined cloud height regimes.

3. RESULTS

3.1 MODIS Collections 5 and 6 Cloud Water Path

The following sections describe the results of using the space-time gridding (STG) algorithm to create custom Level 3 Aqua Moderate-resolution Imaging Spectroradiometer (MODIS) cloud water path (CWP) datasets from the MODIS Collection 5 (C5) and Collection 6 (C6) Level 2 datasets. At the time of this paper, MODIS C5 was the latest complete dataset produced, and processing of MODIS C6 is nearly complete. MODIS C6 has some improved algorithms for cloud detection and retrieval products, and some parameters, such as cloud top pressure (CTP), are available in a higher resolution. Thus, this study analyzes the differences in cloud products between the two collections, and takes into consideration the different CTP resolutions that are provided in the C6 dataset. The MODIS data time period used in this study is over the month of May for the years 2003 - 2012.

3.1.1 Collection 5

Figure 3.1 shows the C5 time-series average for the month of May for the years 2003 - 2012 of the CWP separated into liquid water path (LWP) and ice water path (IWP) for both the confidence and uncertainty-quality cases (see section 2.1.1 for filtering setup). Even with a fairly stringent uncertainty filter value, there are lower CWP values, especially for the IWP in the southern hemisphere storm track, for the uncertainty case compared to the confidence case. This is not surprising given that the southern hemisphere storm track region is difficult for cloud phase retrievals as there are many mid-level and potentially mixed-phase clouds present.

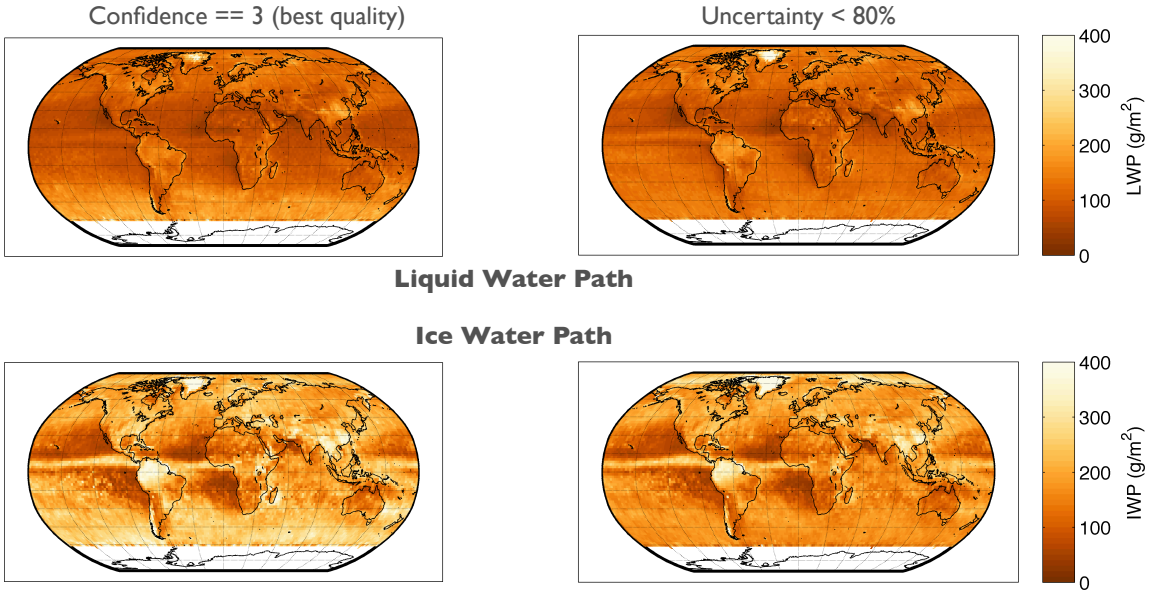

Figure 3.1: Filtered and gridded Aqua MODIS C5 CWP for all clouds (i.e., no height filters) separated into liquid water path (LWP; top) and ice water path (IWP; bottom) for two Level 2 product assessments of quality: (left) best confidence and (right) 80% uncertainty-quality flag cases for the month of May during the years 2003 to 2012.

3.1.2 Collection 6

The two differences between C5 and C6 that most greatly affect this study are the changes in quality assessment and CTP resolution. MODIS C6 has an improved pixel-level retrieval uncertainty algorithm that is to be used in place of the quality assurance bits (i.e., the "confidence" cases). While the quality assurance designation exists in the C6 data files for legacy purposes, it is not meaningful because all cloudy pixels in C6 are assigned to the "best" quality assurance bit. Thus, any C6 confidence case values or figures shown here represent all retrieved cloudy pixels (i.e., no quality filtering). Because of this, the C6 and C5 comparisons discussed in later sections will focus on the uncertainty-quality case.

Figure 3.2 shows the C6 time-series average CWP for all clouds for both the no-quality-filtering case and the uncertainty-quality case. There is little difference in the LWP when the uncertainty quality filter is applied. The effect of the uncertainty quality filter is better seen in the reduction of IWP in the southern hemisphere storm track region, and in the increase in IWP in the northern high latitudes. Similar to the C5 results, the uncertainty case reduction in the southern hemisphere storm track region is likely due to the high uncertainty associated with very thick cloud decks, especially if they're comprised of mid-level and mixed-phase clouds. Additionally, MODIS tends to have high uncertainty with thin ice clouds. Thus, the increase in the northern polar region CWP might be due to the filtering out of thin ice clouds, leaving thicker cloud retrievals to make up the grid cell average.

Figure 3.3 displays side by side the official MODIS C6 Level 3 product with the C6 uncertainty case product for the same time period. Although the customized product is on a coarser grid, there are the same spatial patterns, a similar range of values for the LWP, but lower values in the customized IWP product, mainly in the storm track regions where high uncertainty is likely due to the presence of thick and mid-level, mixed-phase clouds. The differences between the two quality cases, and the differences with the official MODIS Level 3 product, show the impact of the filtering, gridding, and aggregating strategies chosen, and how they must be well thought out to address the science question at hand, and must be well-documented so that others may reproduce and critique the process.

The MODIS C6 dataset has a new 1-km resolution CTP variable, along with a legacy 5-km resolution CTP variable (Menzel et al., 2013; Baum et al., 2012). The new 1-km resolution CTP retrieval algorithm incorporates surface emissivity and an improved IR-phase algorithm. These changes improve detection of low clouds, especially in typical marine stratocumulus areas where a temperature inversion made

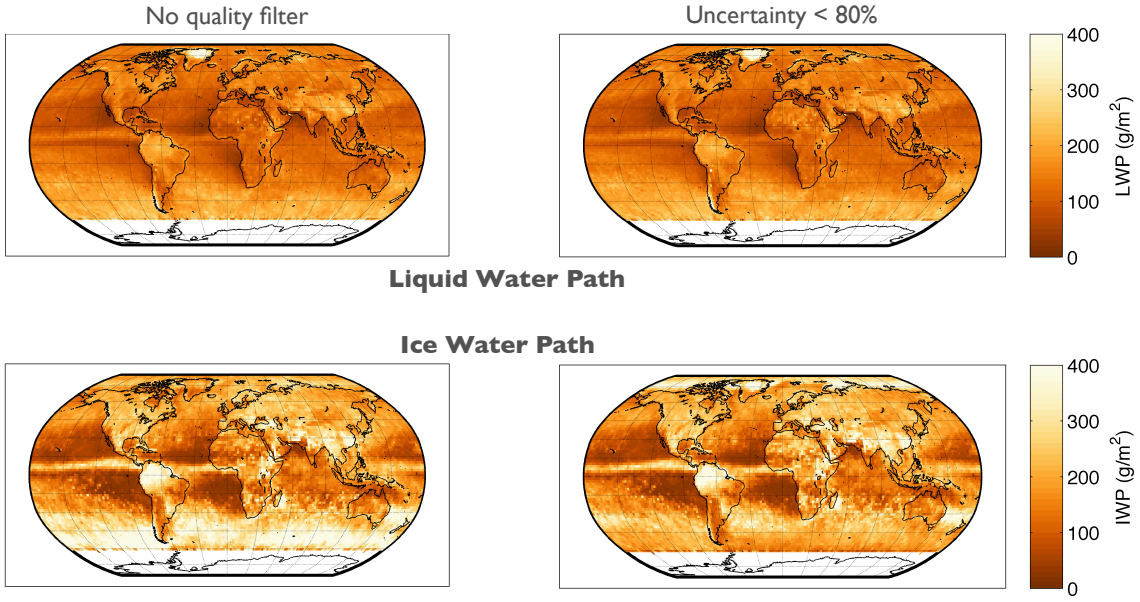

Figure 3.2: Filtered and gridded Aqua MODIS C6 CWP for all clouds (i.e., no height filters) separated into liquid water path (LWP; top) and ice water path (IWP; bottom) for two Level 2 product assessments of quality: (left) no-quality-filter and (right) 80% uncertainty-quality flag case for the month of May during the years 2003 to 2012.

retrievals problematic before, as well as reduced uncertainty of retrievals over desert and icy landscapes, where the high land albedo makes retrievals more uncertain. These changes were not fully implemented in the C6 5-km resolution CTP algorithm; thus, the C6 5-km resolution CTP remains in the dataset mainly for legacy purposes only and is not very different from the C5 dataset. Recall that the CTP in MODIS C5 is available only at 5-km resolution. Since the STG filtering uses CTP to assign height values to the CWP pixels, this study analyzes how the C6 1-km resolution and 5-km resolution CTP differ from one another, and how that affects the vertical distribution of CWP averages.

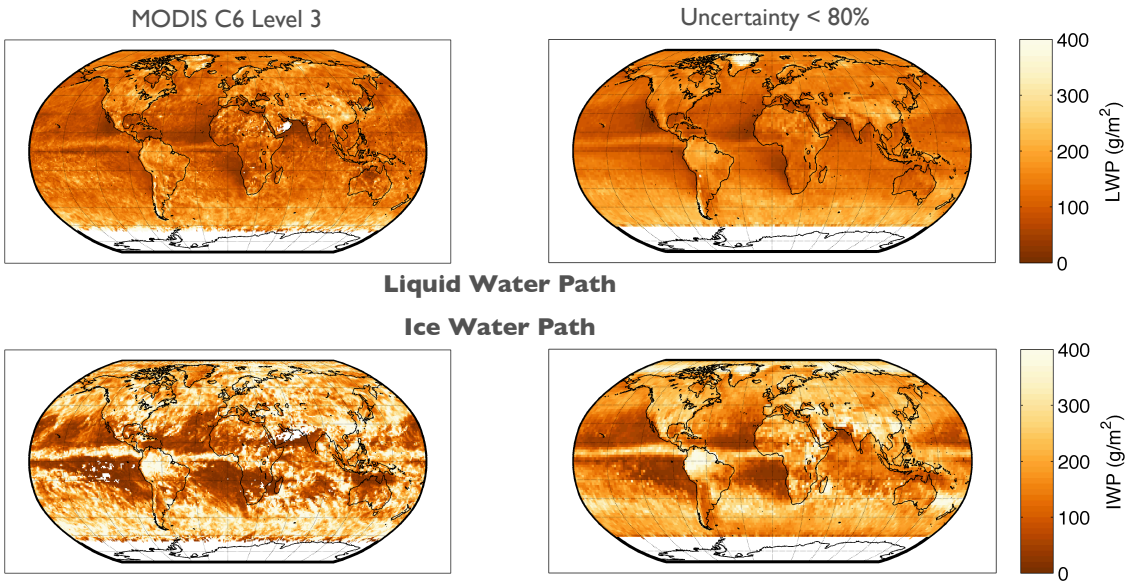

Figure 3.3: (Left) Official MODIS C6 Level 3 product, and (right) filtered and gridded Aqua MODIS C6 CWP for all clouds (i.e., no height filters) separated into liquid water path (LWP; top) and ice water path (IWP; bottom) for the uncertainty-quality case for the month of May during the years 2003 to 2012.

3.1.2.1 C6 cloud top pressure resolution differences

Using the STG algorithm, the MODIS C6 daily CTP pixels for each resolution case are collected into each $2^\circ \times 2^\circ$ grid cell, filtered per an index of the CWP quality and height case filters, and averaged. Figure 3.4 shows the average CTP and difference for the all-clouds height case and uncertainty-quality case. There is little CTP difference over the ocean regions for liquid clouds, with the 1-km resolution CTP showing up to about 100 hPa larger CTP values (i.e., clouds lower in the atmosphere) in the extratropical regions. Over land, the CTP differences are seen mainly over desert regions where the surface emissivity incorporation in the new 1-km resolution CTP product is likely having an effect. The majority of CTP values for ice clouds are much larger in the 5-km resolution case for most of the globe. Generally, it is

seen for the new 1-km resolution CTP that the high clouds (mostly ice clouds) are higher and the low clouds (mostly liquid water clouds) are lower compared to the 5-km resolution CTP. These CTP average difference patterns for both liquid water and ice clouds are similar for both the no-quality-filter case (not shown) and the uncertainty-quality case, meaning that applying the uncertainty quality filter does not greatly affect the overall CTP values.

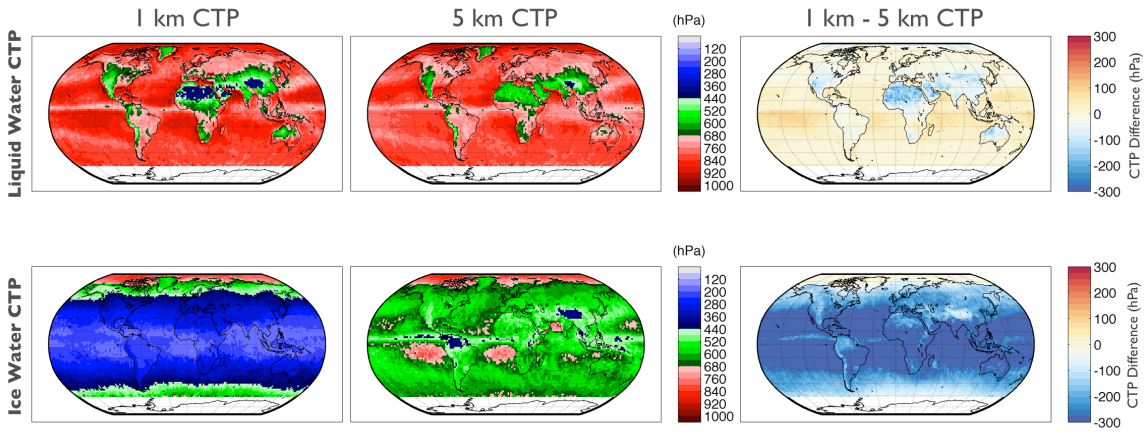

Figure 3.4: MODIS C6 cloud top pressure (CTP) and difference (1-km resolution - 5-km resolution) for all clouds (i.e., no cloud height regime filtering) in the uncertainty-quality case, separated into liquid water path (LWP; top) and ice water path (IWP; bottom) for the month of May during the years 2003 to 2012.

Breaking the CTP down by height regimes shows where these different CTP resolutions may affect the vertical distribution of CWP after being processed by the the STG algorithm. Figure 3.5 shows the global CTP differences (1-km resolution - 5-km resolution) for the uncertainty-quality case. The blue colors in the high cloud regime difference indicate where the 1-km CTP values are smaller (i.e., higher in the atmosphere) than the 5-km CTP; these are most obvious in the extratropical regions.

For the mid-level height regime, CTP values are similar between the 1-km and 5-km resolutions for the liquid clouds, with 1-km CTP again having slightly smaller values (higher clouds) in the extratropical regions. This extratropical difference is more pronounced for the ice cloud pressure values, with the addition of the 1-km CTP having slightly larger (i.e., lower in atmosphere) values within the ITCZ region. In the low cloud regime, the difference between 1-km and 5-km CTP is small for the liquid clouds. For low ice clouds, the 1-km CTP values are overall larger mainly in the extratropical regions.

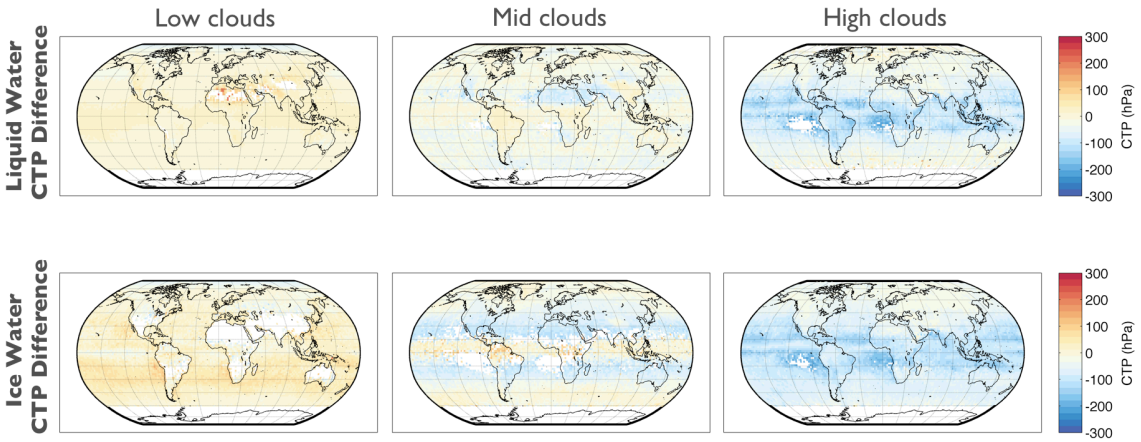

Figure 3.5: MODIS C6 cloud top pressure (CTP) difference (1-km resolution - 5-km resolution) for low, mid, and high height regimes in the uncertainty-quality case, separated into liquid water path (LWP; top) and ice water path (IWP; bottom) for the month of May during the years 2003 to 2012.

Table 3.1 lists the global average CTP values and differences for each height regime for both C6 and C5. The last column shows that the 5-km CTP in both C5 and C6 are not very different for the high and mid-level clouds, but that C6 produces slightly lower low-level clouds. The differences between the 1-km resolution CTP in

Table 3.1: Global average C6 and C5 CTP values and differences (hPa) for (a) liquid clouds and (b) ice clouds under the uncertainty-quality case. Square brackets indicate C6 horizontal CTP resolution in km. Percent differences are relative to dataset being subtracted. All values rounded to nearest whole number.

a. Liq. clouds

Height Regime	C6[1]	C6[5]	C5	(C6[1]-C6[5])	(C6[1]-C5)	(C6[5]-C5)
All	735	732	711	3 (0%)	25 (4%)	21 (3%)
High	305	368	371	-63 (-17%)	-67 (-18%)	-3 (-1%)
Mid	531	559	561	-28 (5%)	-25 (-4%)	-3 (-1%)
Low	819	810	767	9 (1%)	46 (6%)	38 (5%)

b. Ice clouds

Height Regime	C6[1]	C6[5]	C5	(C6[1]-C6[5])	(C6[1]-C5)	(C6[5]-C5)
All	303	562	524	-259 (-46%)	-221 (-42%)	38 (7%)
High	246	323	326	-77 (-24%)	-79 (-24%)	-3 (-1%)
Mid	477	521	515	-44 (-8%)	-33 (-6%)	6 (1%)
Low	763	741	707	22 (3%)	51 (7%)	28 (4%)

C6 and the 5-km resolution CTP for C6 and C5 indicate that the new 1-km CTP retrieval algorithm is measuring higher high clouds, higher mid-level clouds, and lower low clouds for both the liquid water and ice cloud phases. This is likely not only due to the increased horizontal resolution, but also due to the algorithm improvements in detecting thin ice clouds and low stratocumulus clouds beneath a temperature inversion.

For all of these height cases, the C6 CTP differences are similar between the no-quality-filtering case (not shown) and the uncertainty-quality case, meaning that applying the uncertainty quality filter does not greatly affect the CTP values in the different height regimes.

3.1.2.2 C6 cloud water path differences by cloud top pressure resolution

When using either the 1-km or 5-km C6 CTP to assign height values to CWP, there is no difference in CWP for the all-clouds case (Fig. 3.2). The differences in CWP between the resolutions show up when CWP is separated into the different height regimes (Fig. 3.6, Table 3.2). With high clouds, the 5-km CTP assignments produce much larger values of both LWP and IWP, especially in the storm track regions, with global average differences (1-km - 5-km) of -124 g m^{-2} and -107 g m^{-2}, respectfully, amounting to roughly a 40% decrease in each phase for the CWP assigned by 1-km CTP relative to the CWP assigned by 5-km CTP values. In contrast, the mid clouds show larger LWP values (+53 g m^{-2}, or 28%, globally) in the southern hemisphere storm track region and larger IWP values (+145 g m^{-2}, or 113%, globally) in both storm track regions when the CWP heights are assigned by the 1-km CTP values. The main low cloud difference is seen by the somewhat larger IWP values in the southern hemisphere storm track region when using the 5-km CTP values, and this is more pronounced in the no-quality-filter case (not shown) than the uncertainty-quality case. This produces a global average difference (1-km - 5-km) for the low ice clouds of -20 g m^{-2} (-29%), and the low liquid clouds of -7 g m^{-2} (-7%).

It is seen from both this and the previous subsection that the algorithm changes that were made to produce the higher resolution 1-km CTP are changing the distribution of cloud heights, and thus, as these 1-km CTP heights are assigned to the CWP pixels, smaller amounts of high level CWP and greater amounts of mid-level CWP are produced relative to the 5-km CTP height assignments.

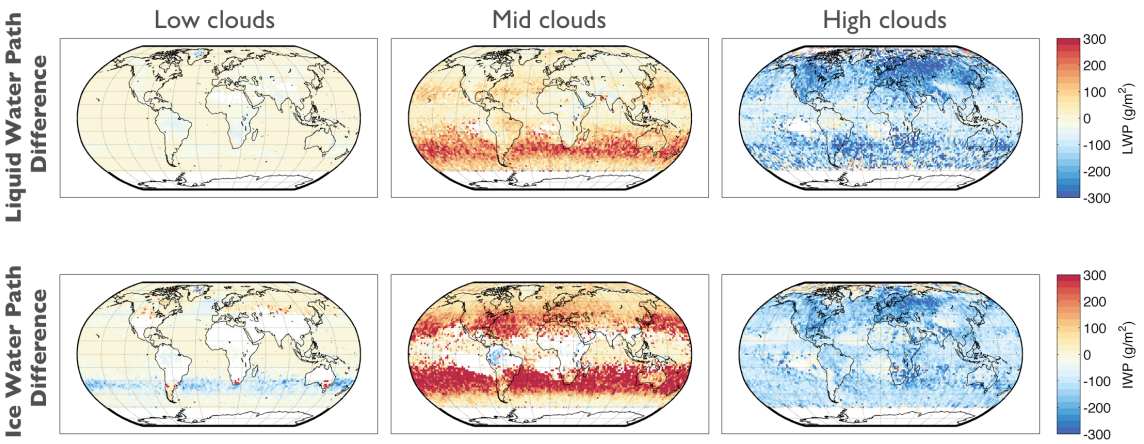

Figure 3.6: MODIS C6 cloud water path (CWP) difference between using 1-km resolution and 5-km resolution cloud top pressure (CTP) height assignments for low, mid, and high cloud height regimes in the uncertainty-quality case, separated into liquid water path (LWP; top) and ice water path (IWP; bottom) for the month of May during the years 2003 to 2012.

3.1.3 Differences between cloud water path in C5 and C6 datasets

The C5 and C6 comparisons in this section focus on only the uncertainty-quality case results since the C6 confidence bits are all set to "best" for legacy purposes only (i.e., C6 confidence case has no quality filter). The total C6 CWP for all clouds (Fig. 3.2) is the same whether using the 1-km or 5-km CTP height assignments. However, when the CWP pixels are assigned heights using the different CTP resolutions, the vertical distribution of CWP within the different cloud height regimes is affected, as was shown in the previous subsection.

Table 3.2 provides the globally averaged CWP values for the uncertainty case in each height regime for C5 and C6, as well as the differences between each collection. The table shows that C6 has a greater amount of LWP than C5 in all height regimes and for each CTP resolution case. C6 produces 115% more mid-level IWP than C5

when using the 1-km CTP height assignment, but almost no difference in the mid-level IWP when using the 5-km height assignment. Additionally, using the 1-km CTP to assign heights to C6 CWP reduces the amount of high and low level IWP in comparison to both C5 and C6 using 5-km height assignments.

Table 3.2: Global average C6 and C5 CWP values and differences (g m^{-2}) for (a) liquid clouds and (b) ice clouds under the uncertainty-quality case. Square brackets indicate C6 horizontal CTP resolution in km. Percent differences are relative to dataset being subtracted. All values rounded to nearest whole number.

a. Liq. clouds

Height Regime	C6[1]	C6[5]	C5	(C6[1]-C6[5])	(C6[1]-C5)	(C6[5]-C5)
All	135	135	111	0 (0%)	24 (22%)	24 (22%)
High	192	316	161	-124 (-39%)	31 (19%)	153 (95%)
Mid	242	189	134	53 (28%)	112 (84%)	55 (41%)
Low	99	106	97	-7 (-7%)	0 (0%)	7 (7%)

b. Ice clouds

Height Regime	C6[1]	C6[5]	C5	(C6[1]-C6[5])	(C6[1]-C5)	(C6[5]-C5)
All	173	173	162	0 (0%)	11 (7%)	11 (7%)
High	174	281	242	-107 (-38%)	-67 (-28%)	40 (17%)
Mid	273	128	127	145 (113%)	146 (115%)	1 (1%)
Low	50	70	84	-20 (-29%)	-35 (-42%)	-15 (-18%)

To see how these global average values are distributed by latitude, Figure 3.7 displays the zonally averaged CWP differences between MODIS C6 and C5, with the C6 CWP heights assigned by the 5-km resolution CTP. The top plot shows that the CWP of liquid high clouds has increased with C6, with a global average increase of 153 g m^{-2}, a 95% increase from C5. The mid-level liquid clouds have also increased in C6 by roughly 55 g m^{-2}, or 41%, globally. The LWP of low clouds, which make up the majority of the liquid water clouds, has changed little between the collections

with a global average increase of 7 g m^{-2}, or 7%, which is seen to be mostly from an increase in LWP in the higher latitudes. On average, the LWP for C6, compared to C5, has increased globally by roughly 24 g m^{-2}, an increase of 22%.

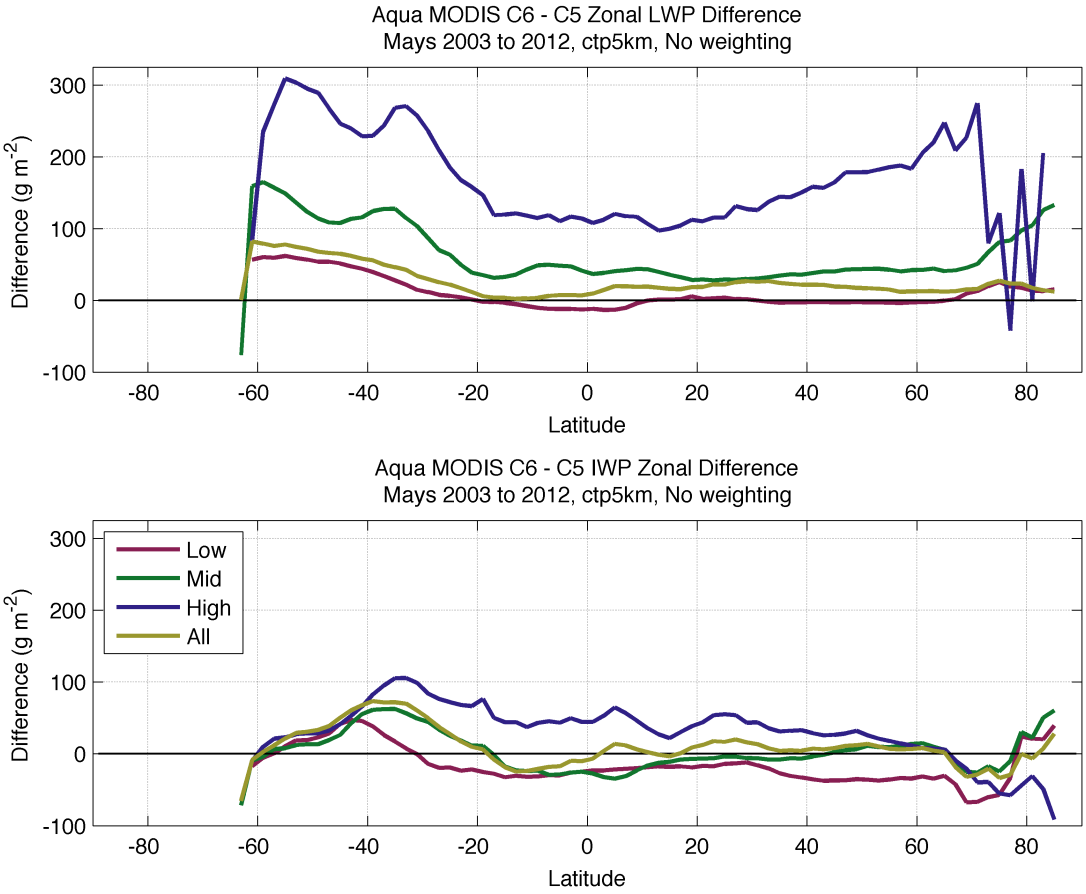

Figure 3.7: Zonally-averaged difference (MODIS C6 - C5) cloud water path for each cloud height regime, with C6 using 5-km resolution CTP height assignments, separated into liquid water path (LWP; top) and ice water path (IWP; bottom) for the month of May during the years 2003 to 2012.

The bottom plot of Fig. 3.7 shows the IWP difference between MODIS C6 using 5-km CTP height assignments and C5. Here the high cloud IWP difference is also

overall increased in C6 by 40 g m^{-2}, or 17%. This increase is mostly seen between the midlatitudes of each hemisphere, with decreases in high ice clouds in the higher latitudes. In contrast, the mid-level ice clouds seem to decrease in C6 between the midlatitudes of each hemisphere while increasing slightly in the higher latitudes. Globally, the average mid cloud IWP is increased in C6 by only 1 g m^{-2}. The low ice clouds in C6 show a slight increase for the higher latitudes, but decreases elsewhere. Overall, the low ice cloud IWP has decreased globally in C6 by 15 g m^{-2}. On average for all C6 ice clouds, there is an increase of 11 g m^{-2}, or 7%, from C5.

Looking now in Fig. 3.8 at the same zonal differences, but with C6 CWP heights assigned by the 1-km resolution CTP, the biggest difference between C6 and C5 is the increase in mid-level CWP. The mid-level LWP peak increased difference of around 300 g m^{-2} is in the southern midlatitudes, with the rest of the latitudes showing an increase of about 50 to 100 g m^{-2}. This gives a globally averaged increase in the C6 mid-level LWP of 112 g m^{-2}, or 84%. There is negligible change with the low level LWP values between the collections. High level LWP is increased in C6, mainly from the tropics through the southern hemisphere, with a global average difference value of 31 g m^{-2}, or 19%. Overall, using the 1-km CTP in C6 to assign LWP heights produces for all clouds a global average increase of 24 g m^{-2}, or 22%, which is the same as using the 5-km CTP to assign C6 CWP heights for the all-clouds case.

The mid-level IWP is increased by 115% in C6 when using the 1-km resolution CTP height assignments, as shown by the bottom plot in Figure 3.8. There is little change in the tropical region, but great increases in the extra tropics through the high latitudes, especially in the southern hemisphere where there is a peak increase around 20°S of roughly 450 g m^{-2}. Low level IWP is decreased in C6 globally by 35 g m^{-2} (-42%), and high level IWP is decreased by 67 g m^{-2} (-28%). Even though there is a dramatic increase in mid-level IWP, the global average difference for all

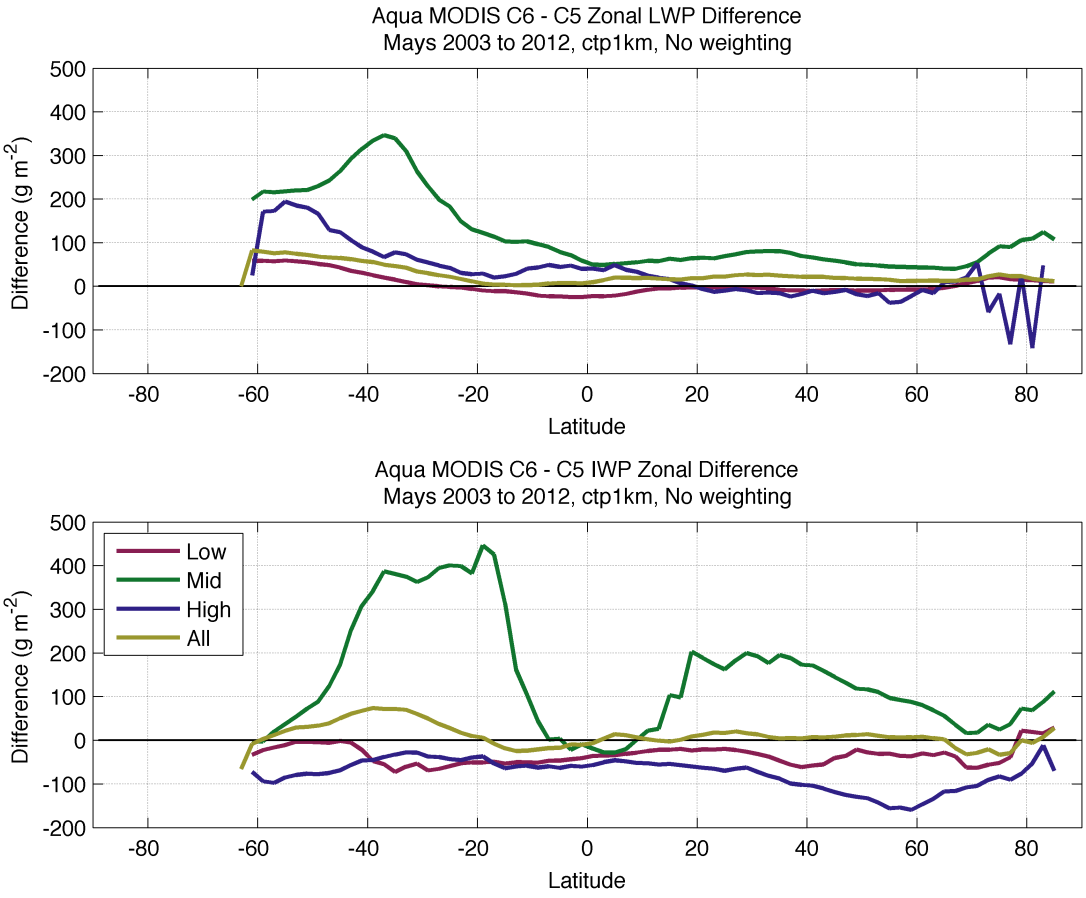

Figure 3.8: Zonally-averaged difference (MODIS C6 - C5) cloud water path for each cloud height regime, with C6 using 1-km resolution CTP height assignments, separated into liquid water path (LWP; top) and ice water path (IWP; bottom) for the month of May during the years 2003 to 2012.

clouds is weighted more by the greater number of high clouds, giving an all-cloud C6 IWP global increase of 11 g m^{-2}, or 7%, from C5.

3.1.3.1 Cloud water path weighted by cloud fraction

Since MODIS CWP values are measurements from only cloudy scenes and the CMIP5 models use both clear and cloudy scene simulations in their CWP calculations, the MODIS CWP has to be weighted by cloud fraction to be compared with

models. The differences in cloud-fraction-weighted CWP between C5 and C6 may affect the results of model-satellite comparisons, depending on which collection is used. Likewise, the CTP resolution (1-km or 5-km) chosen to assign CWP heights for C6 will affect model-satellite comparison results.

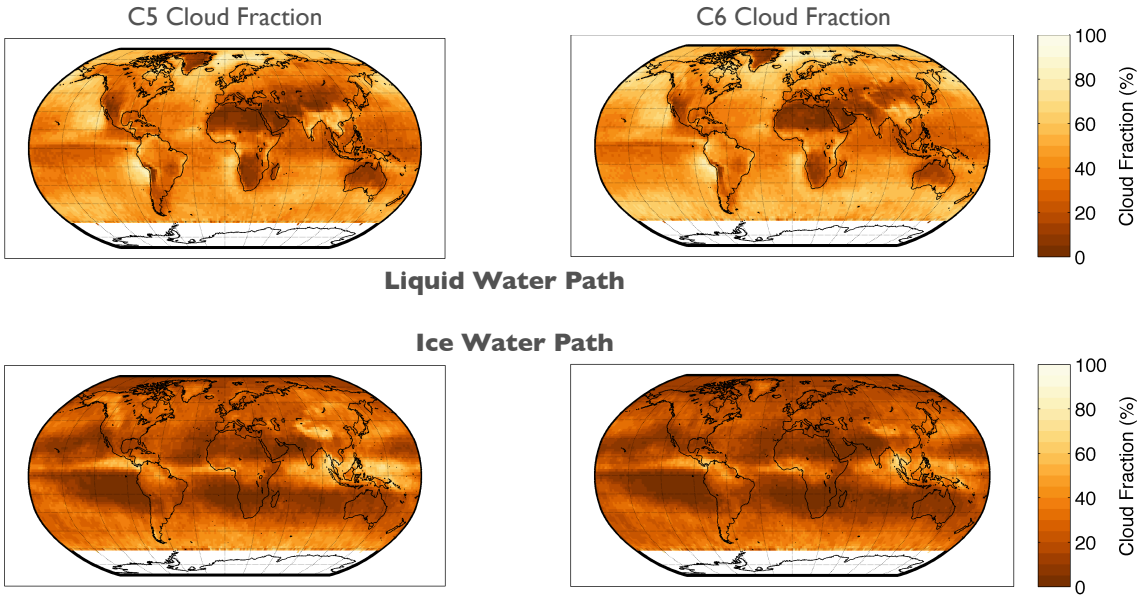

Figure 3.9: (Left) MODIS C5 and (right) C6 cloud fraction for all clouds (i.e., no height filters) separated into liquid water path (LWP; top) and ice water path (IWP; bottom) for the uncertainty-quality case for the month of May during the years 2003 to 2012.

Figure 3.9 shows the cloud fraction for all clouds for C5 and C6 (see section 2.1.1.1 for cloud fraction calculations). The LWP cloud fraction is similar between collections, but there are notable decreases in C6 over Greenland and Australia, and increases over the tropical cyclone track regions, such as over the western Pacific and Indian oceans. The IWP cloud fraction is globally decreased with C6, and is especially low over desert regions, including Australia, northern Africa through

the Middle East, and the southwest region of North America. The C6 changes are likely due to the improved cloud retrieval algorithm which now incorporates surface emissivity and IR cloud phase.

Table 3.3: Global average C6 and C5 cloud-fraction-weighted CWP values and differences (g m^{-2}) for (a) liquid clouds and (b) ice clouds under the uncertainty-quality case. Square brackets indicate C6 horizontal CTP resolution in km. Percent differences are relative to dataset being subtracted. All values rounded to nearest whole number.

a. Liq. clouds

Height Regime	C6[1]	C6[5]	C5	(C6[1]-C6[5])	(C6[1]-C5)	(C6[5]-C5)
All	56	56	47	0 (0%)	9 (19%)	9 (19%)
High	11	10	3	1 (10%)	8 (267%)	8 (267%)
Mid	33	23	19	10 (43%)	14 (74%)	4 (21%)
Low	42	43	40	-1 (-2%)	1 (3%)	3 (8%)

b. Ice clouds

Height Regime	C6[1]	C6[5]	C5	(C6[1]-C6[5])	(C6[1]-C5)	(C6[5]-C5)
All	71	71	74	0 (0%)	-3 (-4%)	-3 (-4%)
High	89	120	112	-31 (-26%)	-22 (-20%)	7 (6%)
Mid	13	26	34	-13 (-50%)	-20 (-59%)	-8 (-24%)
Low	3	4	6	-1 (-25%)	-4 (-67%)	-2(-33%)

Table 3.3 summarizes the global average results of C5 and C6 cloud-fraction-weighted CWP and differences. While the magnitude of the difference values are much smaller compared to the non-weighted CWP, the relative percent differences are overall much greater. This indicates that the way that cloud fraction is calculated has a great impact on the final cloud-fraction-weighted CWP product that is to be used as the observational dataset for comparing to the model simulations of CWP, and so must be carefully considered. For instance, if the cloud fraction calculations are too aggressive, too many clouds will be filtered out (or vice versa), causing a

systematic bias. This study attempts to avoid this problem by using in the cloud fraction calculations both the MODIS cloud mask retrievals, which basically note if a pixel is cloudy or not, and the number of CWP measurements that are kept after going through the STG filtering process.

Fig. 3.10 shows the zonally averaged differences of CWP weighted by cloud fraction between MODIS C6 and C5, with the C6 CWP heights assigned by the 5-km CTP. The magnitude of the high and mid-level liquid water cloud differences are much smaller compared to the unweighted differences. The high liquid water clouds are increased by 8 g m^{-2} in C6, and the mid-level water clouds are increased by 4 g m^{-2}. The C6 low water clouds show an increase of 30 to 40 g m^{-2} in the southern mid to high latitudes, with little change elsewhere, making a global low level average C6 increase of 3 g m^{-2}. The overall global average C6 cloud-fraction-weighted LWP difference is 9 g m^{-2}, an increase of 19% from C5 cloud weighted LWP.

The cloud-fraction-weighted IWP differences between C6 using 5-km CTP height assignments and C5, displayed in the bottom plot of Figure 3.10, show the ice clouds overall decreasing with C6, with the exception of an increase in the high level ice clouds in the southern mid to high latitudes. This produces a globally averaged difference of 7 g m^{-2} for the high cloud-fraction-weighted IWP. The low IWP is decreased by 2 g m^{-2}, and the mid-level IWP is decreased by 8 g m^{-2}. There is a dip in values around 75°N due to a decrease in IWP values for all cloud height regimes over Greenland in C6, which contributes to the globally averaged decreased values for the majority of the height regimes. A greater number of cloudy pixels were not filtered out over Greenland with the C6 dataset, likely due to the algorithm improvements and reduced uncertainty, and a smaller cloud fraction was calculated from these C6 retrievals compared to C5, leading to the dip in IWP values over Greenland.

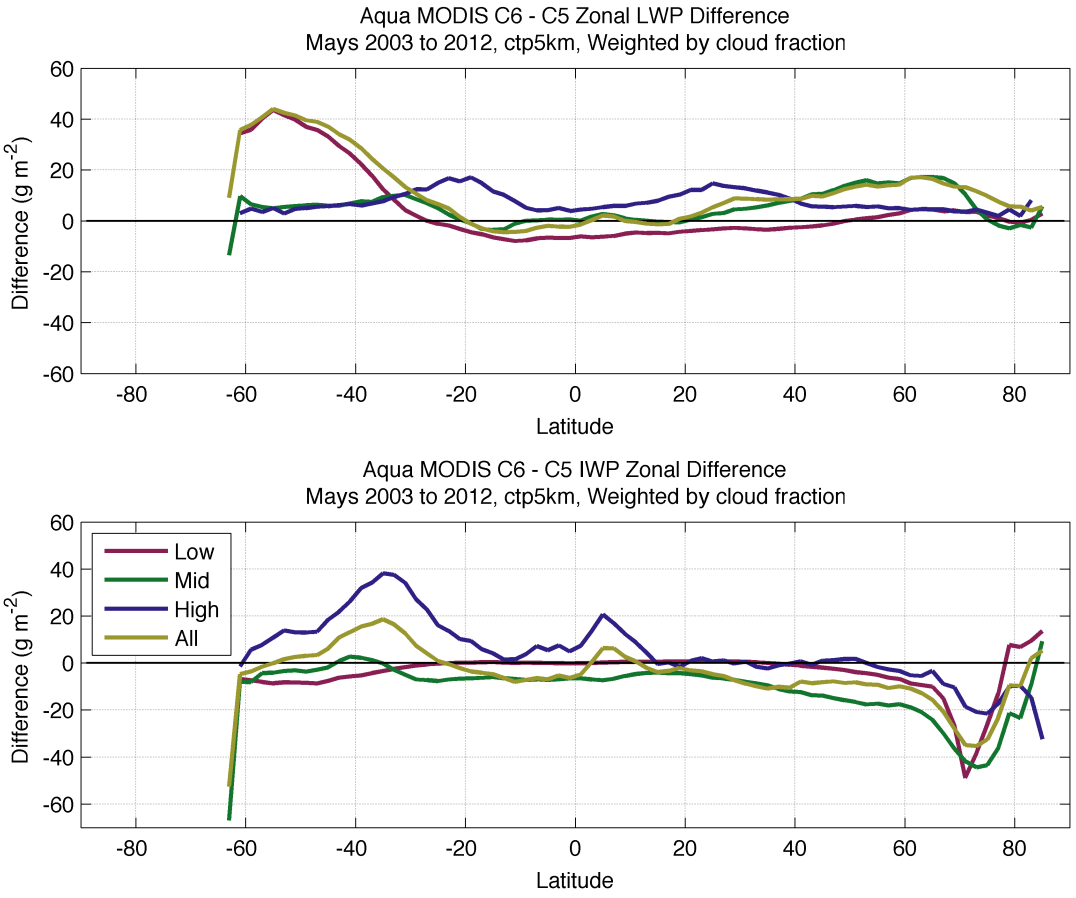

Figure 3.10: Zonally-averaged difference (MODIS C6 - C5) cloud water path, weighted by cloud fraction, for each cloud height regime, with C6 using 5-km CTP height assignments, separated into liquid water path (LWP; top) and ice water path (IWP; bottom) for the month of May during the years 2003 to 2012.

Fig. 3.11 shows the zonally averaged differences of CWP weighted by cloud fraction between MODIS C6 and C5, now with the C6 CWP heights assigned by the 1-km CTP. The low level LWP is slightly decreased in C6 between the midlatitudes, with increases toward the higher latitudes. Because of this, globally averaged low level LWP difference for C6 is negligible at 1 g m^{-2}. The mid-level LWP is increased for C6 throughout most latitudes, with a peak increase of about 40 g m^{-2} around

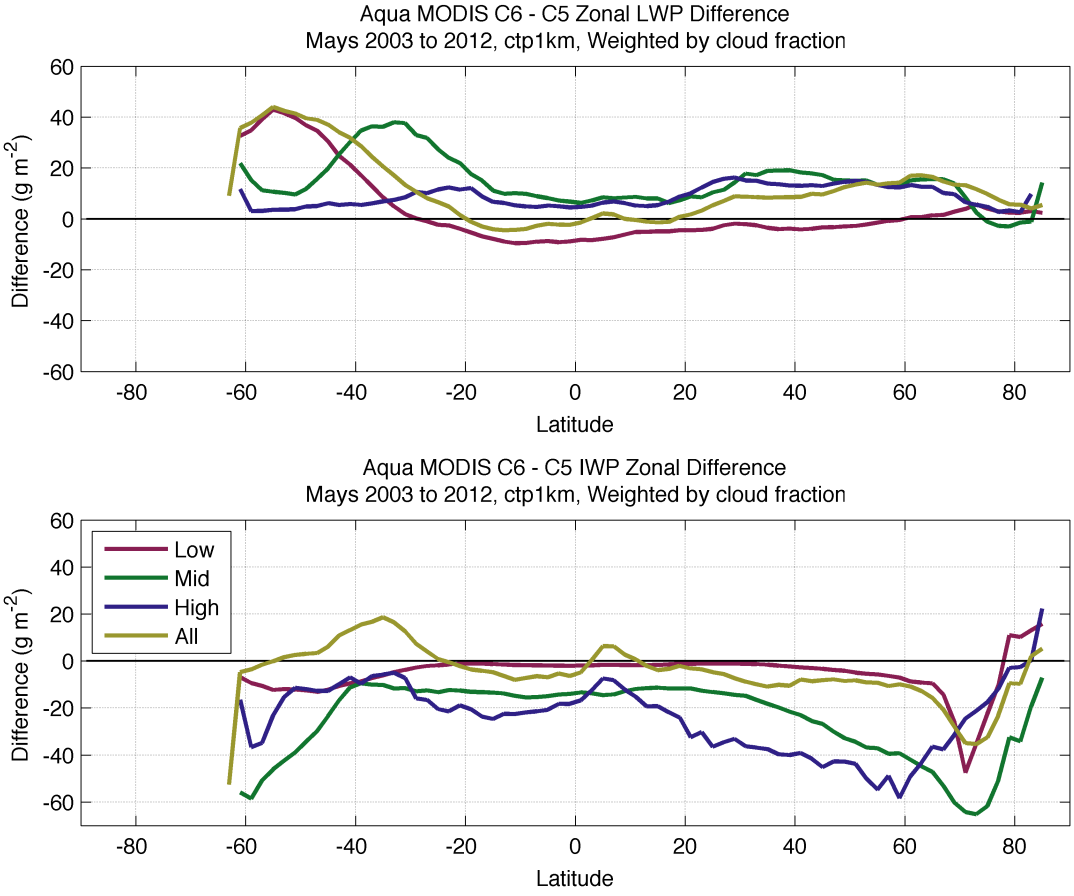

Figure 3.11: Zonally-averaged difference (MODIS C6 - C5) cloud water path, weighted by cloud fraction, for each cloud height regime, with C6 using 1-km CTP height assignments, separated into liquid water path (LWP; top) and ice water path (IWP; bottom) for the month of May during the years 2003 to 2012.

35°S, which is where there is usually high uncertainty within the southern hemisphere storm track region. This is the main LWP difference between the different CTP resolutions in assigning C6 CWP heights in these cloud-fraction-weighted cases, probably due to the 1-km algorithm improvements that have reduced uncertainty in cloud retrievals compared to C5, but that could not be fully implemented in the 5-km CTP retrieval algorithm. The mid-level LWP is increased globally by 14 g m^{-2}, and

the high cloud LWP is increased globally by 8 g m^{-2}. Overall, the global average increase in C6 LWP for cloud-fraction-weighted CWP is 9 g m^{-2}, or a 19% increase from C5 cloud-fraction-weighted LWP, which, again, is the same for the all-clouds case of cloud-fraction-weighted LWP assigned by 5-km CTP.

The cloud-fraction-weighted IWP differences between C6 and C5, using the C6 1-km CTP to assign heights, is shown in the bottom plot of Figure 3.11. There is an overall decrease in C6 cloud-fraction-weighted IWP for all height regimes. There is a decrease in low level IWP of 4 g m^{-2}, a decrease of 20 g m^{-2} for the mid-level IWP, and a decrease of 22 g m^{-2} for the high level IWP. The all-clouds case has a global average reduction in IWP of 3 g m^{-2}, or 4%.

In general, when comparing C6 to C5 CWP that is weighted by cloud fraction, there are increases in C6 LWP, and overall decreases in C6 IWP, no matter the CTP resolution. The C6 CWP is the same for the all-clouds case whether using the 1-km or 5-km CTP height assignments; however, the change in CTP resolution affects how the CWP is distributed vertically. The relatively small changes in the global average CWP values for the all-clouds case are made up from larger relative percent changes within the different height regimes. Regardless of the larger individual height regime differences, the all-clouds average for each cloud phase is dominated by the fraction of clouds in each height regime. For instance, the LWP is composed mainly of low level clouds, and the IWP is composed of mainly high clouds, so the 267% increase in high level LWP and the 67% decrease in low level IWP are not going to have a large effect on the globally-averaged values.

3.2 MODIS Comparisons with Models

To compare Aqua MODIS observations with the GISS-E2-H model, this study uses MODIS C6 CWP that has been weighted by cloud fraction, as described in

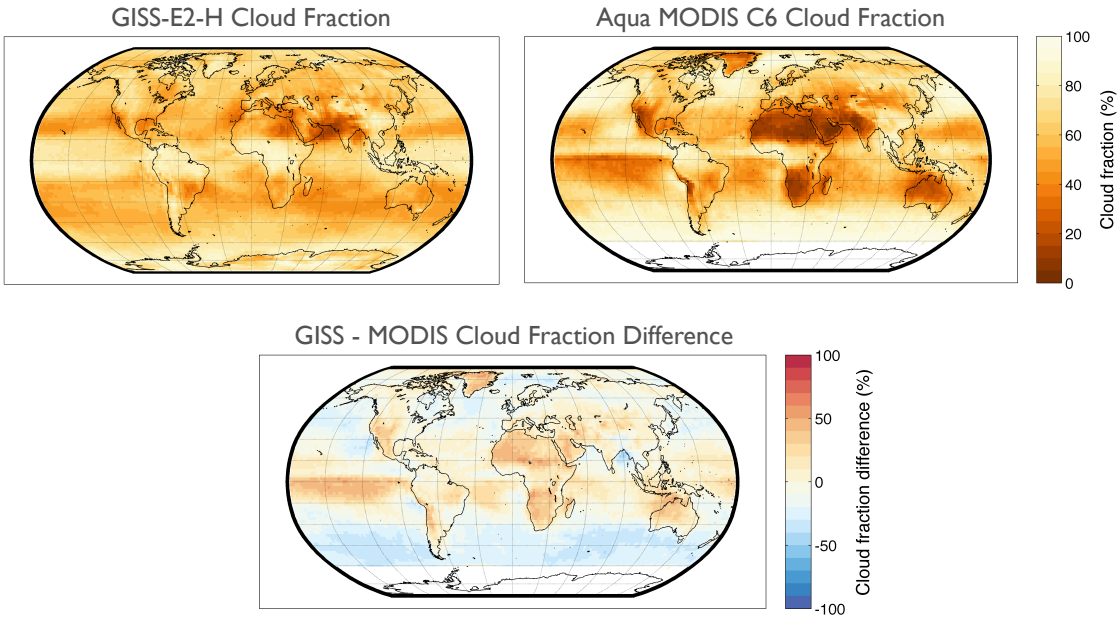

Figure 3.12: Total cloud fraction for all clouds (i.e., no height filters) for the GISS-E2-H model historical run (top left), the filtered and gridded Aqua MODIS C6 uncertainty-quality flag case weighted by cloud fraction (top right), and their difference (bottom) for the month of May during the years 2003 to 2012.

section 2.1.1.1, with CWP pixel heights assigned by the 1-km CTP values, and the 80% uncertainty quality filter applied. To first see how the calculated MODIS cloud fraction compares to the model cloud fraction, the MODIS cloud fraction in the two phases must be combined to make a total cloud fraction since the model only provides a total cloud fraction parameter. Figure 3.12 shows the total cloud fraction for GISS-E2-H, MODIS C6, and the difference between them. While the model and satellite cloud fraction plots show similar spatial features, the MODIS cloud fraction distribution is more variable. The difference plot shows that the GISS model is simulating higher cloud fraction values than MODIS detects in the southern equatorial region and over most continental regions, especially over deserts and Greenland. In contrast, GISS is simulating less cloud fraction in the marine

storm track regions when compared to MODIS. Even with these apparently large spatial differences, the global average values for total cloud fraction are very close at 59% for MODIS and 61% for GISS.

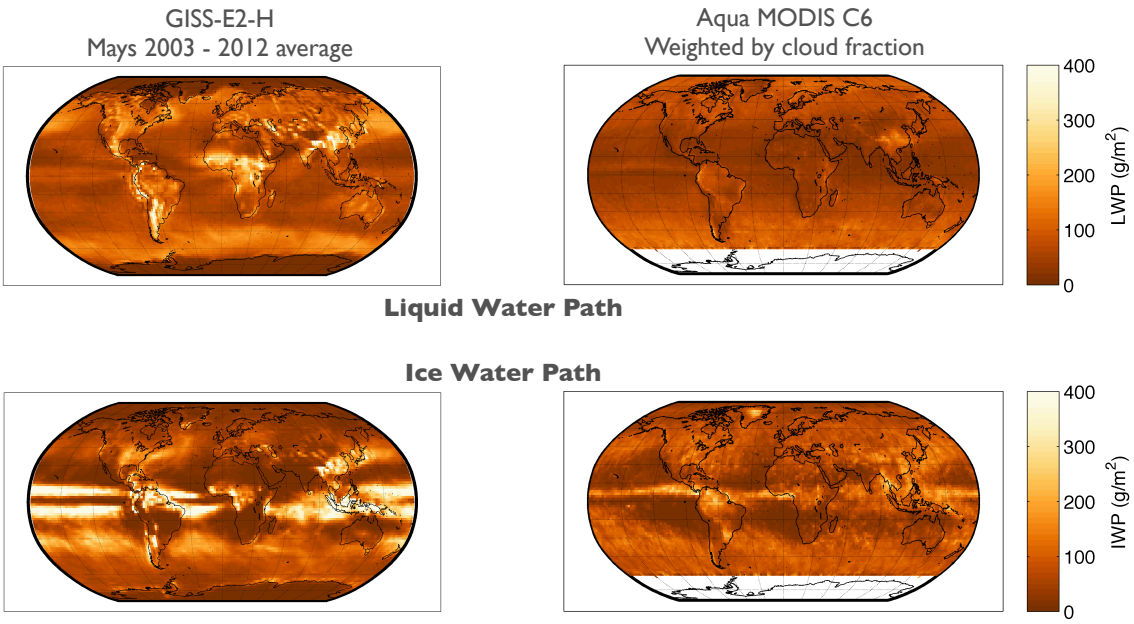

Figure 3.13: CWP for all clouds (i.e., no height filters) separated into liquid water path (LWP; top) and ice water path (IWP; bottom) for the GISS-E2-H model historical run (left) and the filtered and gridded Aqua MODIS C6 uncertainty-quality flag case weighted by cloud fraction (right) for the month of May during the years 2003 to 2012.

Figure 3.13 shows the GISS-E2-H model-simulated CWP for the month of May averaged over the years 2003 - 2012. The original 2 ° latitude by 2.5 ° longitude model grid has been interpolated to be 2 ° by 2 ° to match the custom gridded MODIS C6 satellite product. This model has a double-ITCZ, which can be a problem in coupled models. Globally, the GISS-E2-H average LWP value is 89 g m^{-2}, and IWP is 102 g m^{-2}. Alongside the model plot is the gridded MODIS C6 uncertainty-quality case

product that has been weighted by cloud fraction with a global average LWP of 56 g m^{-2}, and IWP value of 71 g m^{-2}.

Table 3.4: Global average GISS-E2-H and Aqua MODIS C6 cloud-fraction-weighted CWP values (g m^{-2}) and differences (GISS - MODIS), with MODIS C6 using 1-km resolution CTP to assign CWP heights. Percent differences are relative to MODIS. All values rounded to nearest whole number.

	LWP			IWP		
Height Regime	GISS	MODIS	Difference	GISS	MODIS	Difference
All	89	56	29 (59%)	102	71	30 (44%)
High	1	11	-10 (-91%)	74	89	-16 (-17%)
Mid	20	33	-14 (-39%)	9	13	-4 (-31%)
Low	57	42	13 (34%)	2	3	-2 (-33%)

Taking the difference (model - satellite) between the two datasets shown in Fig. 3.13 produces the global difference plots in Fig. 3.14, and the global average and difference values are listed in Table 3.4. In the LWP global difference plot, the mostly red colors show that the model overestimates LWP globally when compared to satellite observations. The IWP difference plot shows that the model greatly overestimates IWP along the ITCZ, but otherwise is comparable or slightly underestimating IWP in higher latitudes. Overall, the model is overestimating CWP globally in both phases by roughly 30 g m^{-2}, or by 59% for LWP and 44% for the IWP, relative to the MODIS measurements. These results are similar to those from Jiang et al. (2012), who found the GISS model to be overestimating both IWP and LWP by about 30 g m^{-2} from the higher end of their observational best estimate ranges of roughly 20 to 70 g m^{-2} for IWP and 30 to 50 g m^{-2} for the LWP. The current study's globally-averaged values of IWP (71 g m^{-2}) and LWP (56 g m^{-2}) are close to the higher end of these best estimate ranges.

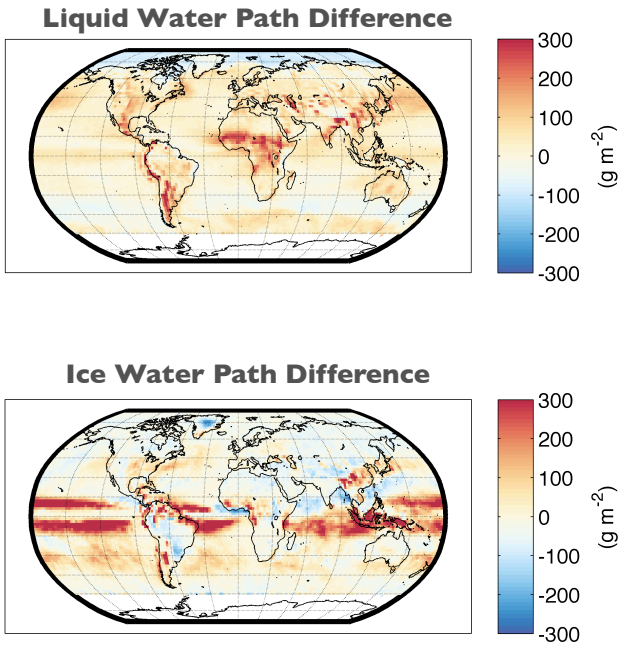

Figure 3.14: CWP global difference (GISS - MODIS C6) for all clouds (i.e., no height filters) separated into liquid water path (LWP; top) and ice water path (IWP; bottom) for the month of May during the years 2003 to 2012.

This global difference is then broken down by height regime to determine where, vertically, these differences between model and observations are occurring. Figure 3.15 shows the global difference plot from Fig. 3.14 separated into low, mid, and high cloud regimes. For low clouds the model is simulating more LWP, especially over land regions and particularly over mountainous regions. This may indicate that convection in the model is too strong over land and is enhancing orographic uplift. The mid-level cloud LWP difference plot also shows that the model simulates slightly more LWP over land regions, but overall the model simulates less LWP than MODIS detects. The difference in mid-level IWP is small. In the high cloud regime MODIS detects greater amounts of IWP overall compared to the model, with the exception of the double ITCZ.

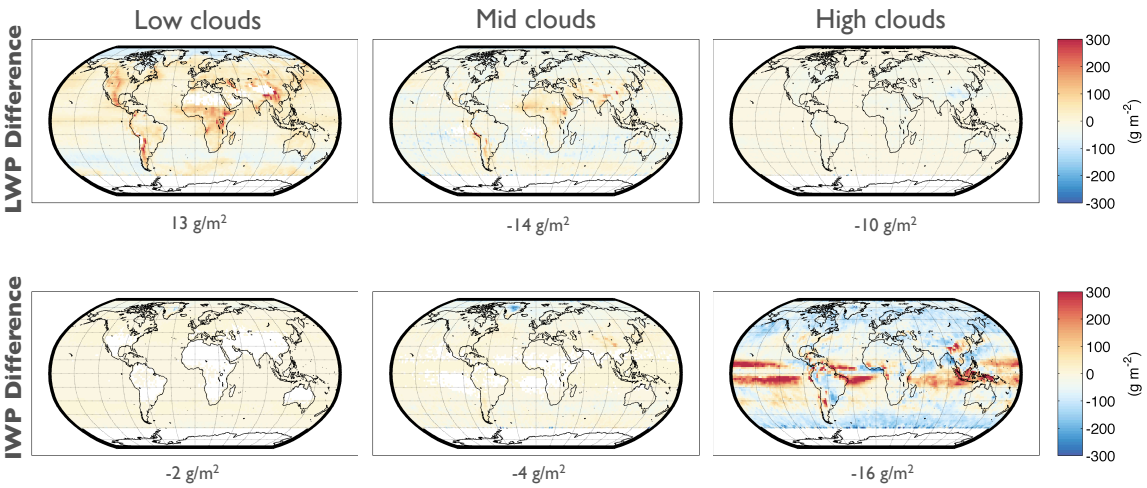

Figure 3.15: CWP global difference (GISS - MODIS C6) for low (left), mid-level (middle), and high (right) clouds separated into liquid water path (LWP; top) and ice water path (IWP; bottom) for the month of May during the years 2003 to 2012. The values under each plot are the global average difference values.

Figure 3.16 shows the zonally-averaged difference by height regime. The main LWP difference is with GISS simulating more low level clouds than MODIS detects. The greatest IWP differences are clearly shown by the GISS model's overestimation of high ice clouds within the double ITCZ area, and lack of high level IWP in higher latitudes. Li et al. (2012) also found through the vertical cloud ice water content information provided by CloudSat/CALIPSO data that the GISS model overestimates IWP most greatly in the high cloud height regime. Overall, these results show that while the model is correctly simulating the global radiation budget, it is getting there through zonally incorrect, yet globally balancing, cloud radiative effects in the high IWP and low LWP regimes.

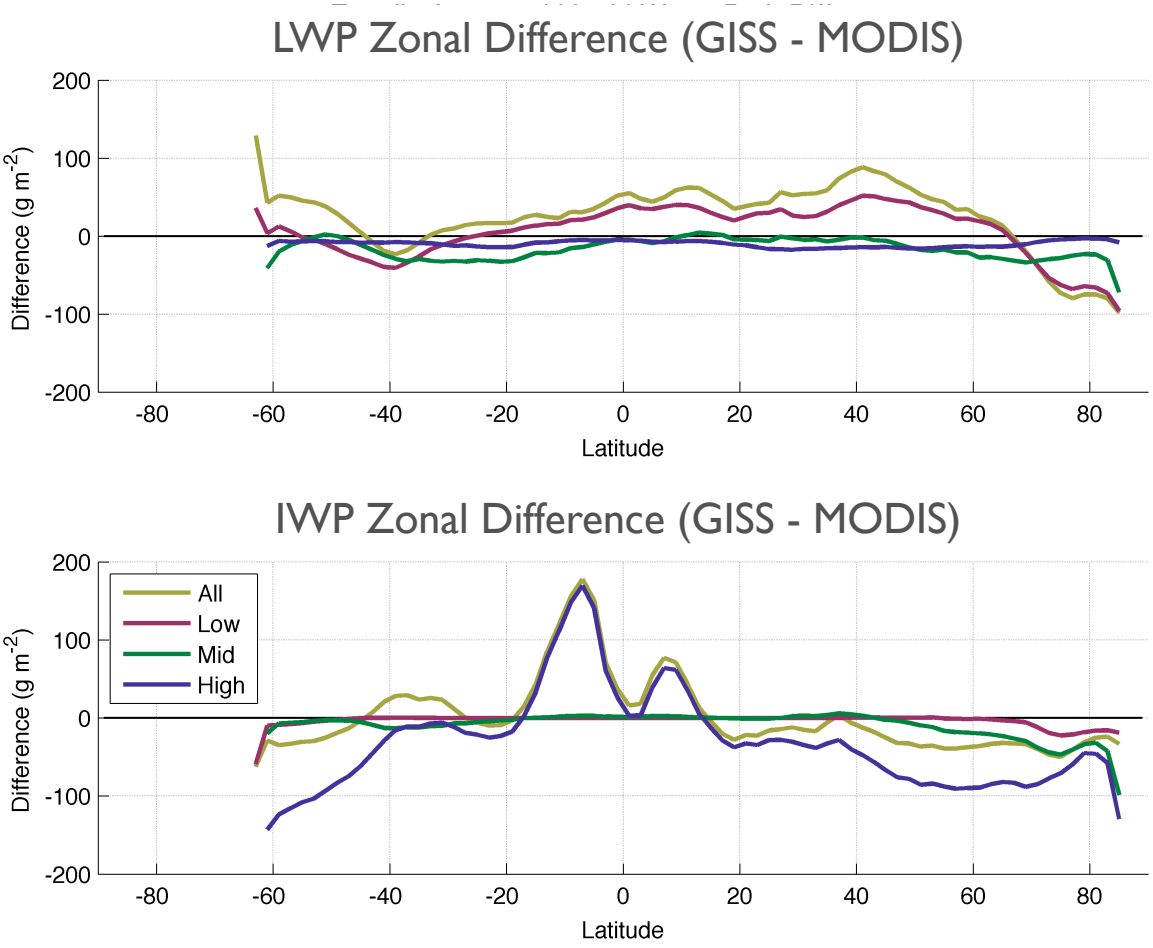

Figure 3.16: Zonally-averaged difference (GISS - MODIS C6) for each cloud height regime separated into liquid water path (LWP; top) and ice water path (IWP; bottom) for the month of May during the years 2003 to 2012.

4. CONCLUSION

4.1 Summary and Conclusions

The results presented here are similar to the results from previous model-satellite comparison work (e.g., Jiang et al. 2012; Li et al. 2012), but were obtained through different methods. These studies assessed differences between global climate model simulations and satellite products such as Moderate-resolution Imaging Spectroradiometer (MODIS) Collection 5 (C5) official Level 3 data, which contain column integrated cloud water path (CWP) data, or Cloud-Aerosol Lidar and Infrared Pathfinder Satellite Observation (CALIPSO) and CloudSat Level 3 data, which can be used to estimate cloud water content at different vertical levels by removing hydrometeors from the total water content values retrieved. MODIS is a well-calibrated instrument with over a decade of retrieval data, and MODIS Collection 6 (C6) products have shown improvements over C5, especially when it comes to thin ice cloud retrievals, low stratus cloud retrievals, and cloud retrievals over desert regions (Baum et al., 2012).

By using the Space-Time Gridding (STG) algorithm to assign the MODIS C6 Level 2 cloud retrieval pixels to the retrieved cloud top pressure (CTP) values, this study was able to analyze MODIS data in different cloud height regimes, which is something these previous studies could not do by using the official MODIS Level 3 datasets. This STG methodology was first used to determine how MODIS C5 and C6 differ by height regime, and found the biggest difference to be an increase in the mid-level CWP in C6, especially in the extratropical and storm track regions. Mid-level and potentially mixed-phase clouds tend to cause high retrieval uncertainty, and the improved cloud retrieval algorithm in C6 has resulted in overall reduced

uncertainty from C5; thus, the increase in C6 mid-level clouds is likely due to these C6 algorithm improvements.

The STG algorithm was then used to compare MODIS C6 data to one of the Goddard Institute for Space Studies (GISS) climate models (GISS-E2-H) and showed, similar to previous model-satellite comparison studies, that the GISS model simulates too much high level ice water path (IWP) in a double ITCZ (intertropical convergence zone), which compensates for a lack of high level IWP in higher latitudes while ensuring the global radiation budget is correct. Jiang et al. (2012) used CloudSat and Aqua MODIS C5 datasets to determine best estimate observation ranges for total column (i.e., all-clouds case) IWP and LWP and found the GISS model to overestimate IWP by about 30 g m^{-2} from the higher end of that estimate range (roughly 20 to 70 g m^{-2}). The LWP best estimate range is from 30 to 50 g m^{-2}, with GISS, again, about 30 g m^{-2} higher than the higher end of that range. Li et al. (2012) used three different CloudSat and CALIPSO products to determine cloud IWP from measured total IWP, and calculated a global average value of around 20 g m^{-2}. CloudSat/CALIPSO data provide vertical information, and show that the GISS model starts to overestimate observed ice water content values above 700 hPa, going up into the mid-cloud height regime, but most greatly overestimates ice water content within the high cloud regime.

The current study's values for MODIS C6 globally-averaged LWP (56 g m^{-2}) and IWP (71 g m^{-2}) are near the upper ends of the best estimate ranges from Jiang et al. (2012), and is also finding the GISS model to be globally overestimating both IWP and LWP by roughly 30 g m^{-2}. This study has used the STG to determine vertical information from MODIS data, and has thus calculated similar results to Li et al. (2012), who found, using CloudSat/CALIPSO data, that the IWP overestimation is mainly in the high cloud height regime.

One implication of this study is that the STG algorithm is a convenient tool to define very specific filtering criteria to create globally gridded datasets from satellite data for use in many applications, such as comparisons with different data collections and global model simulations. Although not described in this paper, the author has also successfully used the STG algorithm to compare satellite retrievals of CTP between Aqua MODIS and Suomi National Polar-orbiting Partnership Visible Infrared Imaging Radiometer Suite (NPP VIIRS); thus, the STG can also be used for inter-satellite comparisons. These are examples of research activities that official Level 3 products may not have been designed for. By using the STG algorithm to create custom datasets on the same grid and with the same filtering criteria applied, more direct and applicable satellite data comparisons can be made with this tool, as opposed to using official Level 3 products where the user has no say in the filtering criteria or grid size.

4.2 Future Work

The biggest hindrance to using the STG algorithm with MODIS data is the time it takes to open and close the hundreds of daily Level 2 data files to pull out and save only the desired variables. However, once the filtering part is complete, the space and time gridding parts of the algorithm are very quick to run on a single desktop computer station, and the code is easily changeable as new investigation topics arise. Thus, future work must first entail optimization of the filtering process. Once that is complete, this algorithm would be practical to use for analysis of seasonal or yearly variations over the entire span of MODIS' lifetime, as opposed to being restricted to just one month over a decade as it was in this study.

Given more time, this study would have compared the customized MODIS dataset to the entire suite of CMIP5 model simulations of CWP to provide a more in-depth

analysis of model simulated cloud parameters.

REFERENCES

Baum, B. A., W. P. Menzel, R. A. Frey, D. C. Tobin, R. E. Holz, S. A. Ackerman, A. K. Heidinger, and P. Yang, 2012: MODIS cloud-top property refinements for Collection 6. *Journal of Applied Meteorology and Climatology*, **51 (6)**, 1145–1163, doi:10.1175/JAMC-D-11-0203.1.

Bony, S., M. Webb, C. Bretherton, S. Klein, P. Siebesma, G. Tselioudis, and M. Zhang, 2011: CFMIP: Towards a better evaluation and understanding of clouds and cloud feedbacks in CMIP5 models. *CLIVAR Exchanges*, **16 (2)**, 20–23.

Boucher, O., et al., 2013: Clouds and aerosols. *Climate Change 2013: The Physical Science Basis. Contribution of Working Group I to the Fifth Assessment Report of the Intergovernmental Panel on Climate Change*, T. Stocker, D. Qin, G.-K. Plattner, M. Tignor, S. Allen, J. Boschung, A. Nauels, Y. Xia, V. Bex, and P. Midgley, Eds., Cambridge University Press, Cambridge, United Kingdom and New York, NY, USA, chap. 7, 571–657.

Cesana, G. and H. Chepfer, 2012: How well do climate models simulate cloud vertical structure? A comparison between CALIPSO-GOCCP satellite observations and CMIP5 models. *Geophysical Research Letters*, **39 (20)**, L20 803, doi:10.1029/2012GL053153.

Dolinar, E., X. Dong, B. Xi, J. Jiang, and H. Su, 2014: Evaluation of CMIP5 simulated clouds and TOA radiation budgets using NASA satellite observations. 1–19, doi:10.1007/s00382-014-2158-9.

ESGF, 2014: Earth System Grid Federation CMIP5 Data Portal. [Available online at `http://pcmdi9.llnl.gov/esgf-web-fe/`].

Flato, G., et al., 2013: Evaluation of climate models. *Climate Change 2013: The*

Physical Science Basis. Contribution of Working Group I to the Fifth Assessment Report of the Intergovernmental Panel on Climate Change, T. Stocker, D. Qin, G.-K. Plattner, M. Tignor, S. Allen, J. Boschung, A. Nauels, Y. Xia, V. Bex, and P. Midgley, Eds., Cambridge University Press, Cambridge, United Kingdom and New York, NY, USA, chap. 9, 741–866.

GSFC, 2014: LAADS Web: Level 1 and Atmosphere Archive and Distribution System. [Available online at `http://ladsweb.nascom.nasa.gov/`].

Jiang, J. H., et al., 2012: Evaluation of cloud and water vapor simulations in CMIP5 climate models using NASA "A-Train" satellite observations. *Journal of Geophysical Research*, **117**, D14 105.

Li, J. L. F., et al., 2012: An observationally based evaluation of cloud ice water in CMIP3 and CMIP5 GCMs and contemporary reanalyses using contemporary satellite data. *Journal of Geophysical Research*, **117 (16)**, D16 105, doi:http://dx.doi.org/10.1029/2012JD017640.

Menzel, W. P., R. A. Frey, and B. A. Baum, 2013: Cloud Top Properties and Cloud Phase Algorithm Theoretical Basis Document: Collection 006 Update, version 10. [Available online at `http://modis-atmos.gsfc.nasa.gov/_docs/MOD06_ATBD_2013_03_06.pdf`], 70 pp.

MODIS Atmosphere, 2014: Release of MODIS/Aqua Collection 6 Level-2 Aerosol, Cloud, and other Products. [Available online at `http://modis-atmos.gsfc.nasa.gov/_docs/C6_MODIS_atmo_L2_announcement_v2.pdf`].

Nam, C., S. Bony, J. L. Dufresne, and H. Chepfer, 2012: The 'too few, too bright' tropical low-cloud problem in CMIP5 models. *Geophysical Research Letters*, **39 (21)**, L21 801, doi:10.1029/2012GL053421.

Platnick, S., et al., 2013: MODIS Cloud Optical Properties: Exec. Summary of Collection 6 Level-2 Optical Property Changes for MOD06/MYD06. [Available

online at http://modis-atmos.gsfc.nasa.gov/_docs/C6MOD06OPExecSum.pdf], 6 pp.

Smith, N., W. P. Menzel, E. Weisz, A. K. Heidinger, and B. A. Baum, 2013: A uniform space–time gridding algorithm for comparison of satellite data products: Characterization and sensitivity study. *Journal of Applied Meteorology and Climatology*, **52 (1)**, 255–268, doi:10.1175/JAMC-D-12-031.1.

Stocker, T., et al., (Eds.) , 2013: *Climate Change 2013: The Physical Science Basis. Contribution of Working Group I to the Fifth Assessment Report of the Intergovernmental Panel on Climate Change*. Cambridge University Press, Cambridge, United Kingdom and New York, NY, USA, 1535 pp.

Su, H., et al., 2013: Diagnosis of regime-dependent cloud simulation errors in CMIP5 models using "A-Train" satellite observations and reanalysis data. *Journal of Geophysical Research: Atmospheres*, **118 (7)**, 2762–2780, doi:10.1029/2012JD018575.

Taylor, K. E., R. J. Stouffer, and G. A. Meehl, 2012: An overview of CMIP5 and the experiment design. *Bulletin of the American Meteorological Society*, **93 (4)**, 485–498, doi:10.1175/BAMS-D-11-00094.1.

Tian, B., E. J. Fetzer, B. H. Kahn, J. Teixeira, E. Manning, and T. Hearty, 2013: Evaluating CMIP5 models using AIRS tropospheric air temperature and specific humidity climatology. *Journal of Geophysical Research: Atmospheres*, **118 (1)**, 114–134, doi:10.1029/2012JD018607.